Journal of Chromatography A 1774 (2026) 466853

Contents lists available at ScienceDirect

Journal of Chromatography A

journal homepage: www.elsevier.com/locate/chroma

Archaea synthesize heterochiral phospholipid membranes as revealed by chiral analysis of archaeols

Walter Hofmann [a], Andrea Palyzová [b], Jan Jansa [b], Nika Pende [a], Simon K.-M.R. Rittmann [a], Tomáš Řezanka [b,*]

[a] Archaea Physiology & Biotechnology Group, Department of Functional and Evolutionary Ecology, Universität Wien, Djerassiplatz 1, 1030 Vienna, Austria
[b] Institute of Microbiology, Czech Academy of Sciences, Vídeňská 1083, 142 00 Prague, Czech Republic

ARTICLE INFO

Keywords:
Archaea
Archaeols
Biosynthesis
Diversity
Membrane Lipids
Stereoisomers

ABSTRACT

This study comprehensively characterizes structural diversity of archaeol lipids in selected archaeal genera, integrating available genomic information with advanced lipidomic and stereochemical analyzes. Study of genomes from six archaeal genera revealed the presence of key enzymes involved in glycerophosphate biosynthesis, namely glycerol-1-phosphate dehydrogenase and glycerol-3-phosphate dehydrogenase. Their coexistence in some of the studied strains suggests the ability of these organisms to synthesize both enantiomeric forms of glycerol phosphates. Shotgun lipidomic profiling confirmed the presence of saturated and unsaturated archaeols, including extended forms (C20–C25), hydroxyarchaeols, and tetraether lipids, especially in the species *Haloferax volcanii, Methanopyrus kandleri,* and *Sulfolobus acidocaldarius*. Using on-line 2D LC-MS/MS, a specific molecular species of archaeol (20:3–25:4-AR) with seven double bonds was identified in *H. volcanii*, while bis-extended archaeol (C25–C25) was not detected. Chiral HPLC of a commercial archaeol standard resolved four isomers, with the (*R*)-2,3-di-*O*-phytanyl-*sn*-glycerol stereoisomer being the most abundant (> 80 %). In four of our archaeal strains a minor *S* enantiomer was present at concentrations of 6.8–13.9 % relative to the main *R* isomer, and its presence coincided with the presence of both glycerol phosphate dehydrogenases in the respective genomes. The distribution of these isomers across the studied strains supports the coexistence of both *R*- and *S*-enantiomers of archaeols in some, but not all, archaeal lineages. These findings highlight the stereochemical and structural complexity of archaeal membrane lipids and provide new insights into their biosynthetic diversity.

1. Introduction

The emergence of biological membranes was a pivotal event in early cellular life evolution, allowing compartmentalization, energy conservation, and ultimately the origin of life as we know it. Membranes not only form the fundamental boundary between living cells and their environment but also preserve a molecular record of ancient biochemical pathways. A defining characteristic of this record is the so-called 'lipid divide' between Archaea and Bacteria: Archaeal membranes are built from ether-linked isoprenoid chains attached to *sn*-glycerol-1-phosphate (G1P), while bacterial and eukaryotic membranes consist of ester-linked fatty acids on *sn*-glycerol-3-phosphate (G3P) [1]. Thus, this divide is not only chemical (ether versus ester bonds) but also stereochemical, with profound implications for the evolution of cellular life and the emergence of biological homochirality [2]. Supplementary Fig. S1 demonstrates the structural formulas of the two classes of lipids that differ in the stereochemistry of the glycerol phosphate backbone and the stereochemistry of the glycerol moiety is explicitly indicated.

The origin and timing of this lipid divide remain debated. Genomic and enzymatic evidence suggests that it emerged after the divergence of Archaea and Bacteria, since their respective glycerophosphate dehydrogenases, G1P dehydrogenase (G1PDH, EC 1.1.1.261) in Archaea and G3P dehydrogenase (G3PDH, EC 1.1.5.3) in Bacteria, are not homologous [3,4]. However, experimental studies have shown that heterochiral membranes, composed of G1P and G3P lipids, are stable and functional [5]. This suggests that homochirality fixation was likely driven by selective biochemical interactions or environmental pressures rather than inherent stereochemical incompatibility [6]. For example, *Escherichia coli* engineered with a hybrid heterochiral membrane – where 30 % of total phospholipids were true archaeol-based (G1P) species – exhibited significantly higher tolerance to heat shock (55 °C), survival after freezing at −80 °C, or presence of 2 % butanol in the

* Corresponding author.
E-mail address: rezanka@biomed.cas.cz (T. Řezanka).

https://doi.org/10.1016/j.chroma.2026.466853
Received 26 November 2025; Received in revised form 27 January 2026; Accepted 28 February 2026
Available online 1 March 2026

medium [7].

A common feature of archaeal membranes is the presence of phospho- and glyco-lipids derived from extended ether lipids such as archaeol and glycerol dialkyl glycerol tetraether lipids (GDGTs) [8]. Recent advances in chiral chromatography and high-resolution mass spectrometry (HRMS) have enabled detailed characterization of these lipids, shedding light on the biosynthetic pathways that underpin the lipid divide. These techniques allow the separation and structural elucidation of glycerophosphate (GP) enantiomers [9], providing a window into the early evolution of cellular membranes and facilitating reconstructions of ancient lipid biosynthesis pathways. Understanding how this molecular asymmetry emerged not only clarifies the biology of the last universal common ancestor (LUCA) of both Archaea and Bacteria, but also illuminates how the biochemical foundations of life became firmly established.

In particular, the assumed exclusive use of G1P by Archaea raises important questions about the origins of chirality in lipid metabolism. Was the fixation of homochirality a consequence of selective biochemical interactions or was it shaped by environmental constraints? A commonly accepted hypothesis argues that the chemical stability of ether-linked isoprenoid membranes under extreme conditions, such as those in hydrothermal vents or hypersaline environments, conferred a selective advantage to early Archaea [10].

Archaeol, a diether lipid composed of two phytanyl chains linked at positions *sn*-2 and *sn-3* of glycerol [11], exemplifies this distinct chemistry. Two structural differences distinguish archaeal lipids from those of Bacteria and Eukarya: (i) the use of *sn*-2,3-glycerol instead of *sn*-1, 2-glycerol and (ii) the predominance of ether rather than ester bonds [12]. Natural archaeol has three chiral centers in each isoprenoid chain (positions 3*R*, 7*R*, 11*R*), totaling six per hydrocarbon chains, plus one on the glycerol backbone. This yields 2^7, i.e., 128 possible stereoisomers, along with four additional structural variants: macrocyclic archaeol (with two phytanyl chains forming a 36-membered ring), hydroxylated archaeol, sesterterpanyl archaeol (extended by C25 chains), and unsaturated derivatives containing double bond(s) [13]. Archaeol occurs in all Archaea, although in varying proportions [12]. Together with GDGTs, archaeol constitutes the so-called core lipids, widely used as biomarkers in sediments, freshwater, and marine environments [14]. Their unique structures are believed to underlie archaeal adaptation to extreme habitats [15–17].

The biosynthesis of archaeal side (phytanyl) chains has previously been described in detail [18]. G1P itself is synthesized by reducing glycerone phosphate (3-hydroxy-2-oxopropyl dihydrogen phosphate) by G1PDH. Interestingly, published studies show that both G1PDH and G3PDH are present in certain Archaea [19–21].

Advanced analytical methods have firmly established the stereochemistry of G1P. Chiral chromatography of derivatized GPs in specialized columns, combined with HRMS, enables resolution of GP enantiomers [22,23]. Tandem mass spectrometry (MS/MS) provides diagnostic fragmentation patterns, while high-resolution platforms such as Orbitrap confirm exact molecular structures [24]. These methods confirm not only the exclusive use of G1P in archaeal membranes, but also trace biosynthetic intermediates and degradation products. Geochemical analyses of ancient sediments, interpreted through chiral chromatography and MS, support the antiquity of archaeal membranes in the biosphere of the early Earth [25].

In particular, some Archaea appear to synthesize lipids based on both G1P and G3P, and certain species produce both enantiomers [21]. In *Halobacterium salinarum* and *Pyrococcus* sp., G3P accounted for ~4 % of total GPs, while in *Thermoplasma* sp. strain HO-62 it reached as much as 24 % of total GPs. To further increase our understanding, we performed detailed lipidomic analyses of several Archaea strains with a particular focus on the archaeol stereoisomers.

2. Experimental section

2.1. Chemicals and standards

Common chemicals were purchased from Sigma-Aldrich, Ltd. (now Merck, Prague, Czech Republic), including acetonitrile, 2-propanol, hexane, and dichloromethane. The 999986C Avanti (4ME 16:0 diether DG, i.e. archaeol) and 850356P Avanti (4ME 16:0 PC, archaeol phosphatidylcholine) were purchased from Avanti Polar Lipids (Alabaster, Alabama, USA).

2.2. Cultivation and growth conditions

All archaeal strains were cultivated in batch or closed batch cultivation modes under their species-specific conditions as detailed in the supplementary materials, and harvested at the late-exponential growth phase. All cultures were harvested by centrifugation (2,630 × g), flash-frozen in liquid nitrogen, and freeze-dried for 24 h. A minimum of 15–20 mg of freeze-dried biomass per strain was used for lipid extraction and subsequent chromatographic analyses. The step-by-step lipid analysis process is shown in supplementary Fig. S2.

2.3. Lipid extraction and saponification

The lyophilized samples were extracted using a modified Bligh and Dyer method [26]. Briefly, biomass samples (Supplementary Table S1) were extracted using a mixture of methanol, dichloromethane, and phosphate buffer at pH 7.4 (2:1:0.8, vol:vol:vol). After 10 min of sonication, additional dichloromethane and buffer were added to the mixture to achieve a final ratio of methanol:dichloromethane:buffer of 1:1:0.8 vol:vol:vol. The phases were separated and the extraction was repeated three more times [27].

To preserve the allylic bonds in the core lipids, saponification, rather than acid methanolysis, was used to recover the core lipids from the total lipids obtained by extraction [28]. Total lipids were hydrolyzed for 2 h with 0.5 N KOH in a MeOH/H_2O mixture (3:1, vol:vol) at 75 °C. After cooling, the unsaponified material was extracted with hexane/$CHCl_3$ (4:1, vol:vol), dried over Na_2SO_4 and evaporated to dryness under a stream of N_2. The weight of the unsaponifiable fractions, representing the total core lipids, is given in supplementary Table S1 (for example, *H. volcanii* = 4.58 mg of 168.3 mg of lyophilized cells, corresponding to 2.72 weight %).

2.4. Shotgun analysis

The linear ion trap quadrupole LTQ-Orbitrap Velos mass spectrometer (Thermo Fisher Scientific, San Jose, CA, USA) was equipped with a heated electrospray interface (HESI) operating in positive ionization mode. The mass spectrometer (MS) scan range was set in the Fourier transform (FT) cell and recorded within a window of 200–2000 Da. The mass resolution was set at 105,000 at *m/z* 400, and the ion spray voltage was +3.5 kV in electrospray positive ionization mode (ESI^+). Flow Injection Analysis was used for sample introduction into the heated ESI-MS (H-ESI-MS) ion source. Acetonitrile (ACN) with 5 mmol L^{-1} aqueous ammonium acetate and 2-propanol (iPrOH) with 5 mmol L^{-1} aqueous ammonium acetate (50/50 v/v) was used at a flow rate of 125 µL/min.

The ionization parameters were as follows: N_2 was used as the nebulizer gas, set at 18 arbitrary units for the sheath gas and 7 arbitrary units for the auxiliary gas; ion source temperature was 250 °C; capillary temperature was 230 °C; capillary voltage was 50 V; and the tube lens voltage was 170 V. Helium was used as the collision gas in collision-induced dissociation (CID) experiments. A CID normalization energy of 35 % was applied to fragment the parent ions. The MS/MS product ions were detected in high-resolution FT mode.

The MS was calibrated using a Pierce LTQ Orbitrap positive ion calibration solution (Thermo Fisher Scientific, San Jose, CA, USA).

During mass spectral acquisition, an internal lock mass was used: *m/z* 413.2662 $[M+Na]^+$, corresponding to diisooctylphthalate in ESI^+. The mass accuracy achieved was better than 1.0 ppm. Core lipid structures were confirmed using the LIPID MAPS Lipidomics Gateway spectral database (LIPID MAPS, 2025) and previously published descriptions of positive mass spectra of core lipids [14,27,29–32].

2.5. Analysis of archaeols by two-dimensional on-line LC-tandem MS

Analysis of the core lipids was performed in two modes. In the first mode, reverse phase high-performance liquid chromatography and high-resolution positive electrospray ionization mass spectrometry (RP-HPLC/HR-ESI^+-MS) was employed to determine the retention times of the respective core lipids. In the second mode (chiral LC-MS), the relevant fractions were transferred to the Astec Cyclobond™ column via a Rheodyne valve (see below and supplementary Fig. S3 for details), and the individual peaks were identified using tandem MS and optical rotation.

The HPLC setup consisted of a 1090 Win system, a PV5 ternary pump, and an automatic injector (HP 1090 series, Hewlett Packard, USA), along with three Luna Omega columns (Phenomenex, Aschaffenburg, Germany) (1.6 µm, C18, 100 Å, 150 × 2.1 mm) connected in series. In our setup, the efficiency of ~130,000 plates/meter was achieved. Archaeol from Merck, with a retention time of 37.75 min, was used as an external standard. The flow rate was 0.25 mL min^{-1}, the injection volume was 10 µL, and the column temperature was maintained at 35 °C.

The core lipids were separated using a solvent gradient program. The mobile phase consisted of acetonitrile (ACN) with 5 mmol L^{-1} aqueous ammonium acetate and 2-propanol (iPrOH) with 5 mmol L^{-1} aqueous ammonium acetate. Gradient conditions were as follows: initially, ACN/iPrOH (99:1, vol:vol), then a linear shift to 25:75 ACN/iPrOH (vol:vol) from 5 to 75 min, followed by a 10 min hold. The system was returned to the initial composition for 10 min. Ten percent of the HPLC flow was directed to the LTQ Orbitrap Velos system (see above), while the remaining 90 % of the flow, containing fractions of individual core lipids, was diverted for fraction collection. Time windows of 0.7 min were applied for both archaeol and extended archaeol. Specifically, the interval from 37.38 to 38.08 min for archaeol (C20, C20) and from 47.45 to 48.15 min for extended arachaeol (C20, C25) was transferred via a Rheodyne valve (type 7125, Rohnert Park, CA, USA, MXT715-000), a 2-position 6-port switching valve equipped with a 200 µL stainless steel sample loop, to a second column. A schematic diagram of the automatic column-switching HPLC system used in this study is shown in supplementary Fig. S3.

The second-stage columns, used to separate archaeol and extended archaeol, consisted of two Astec Cyclobond™ I 2000 DMP chiral LC columns (3,5-dimethyl-phenyl-carbamate modified β-cyclodextrin, 5 µm, 250 × 4.6 mm) from Sigma-Aldrich, Ltd., connected in series. The mobile phase gradient was established as follows: starting at 93 % A and 7 % B at 0 min, transitioning to 45 % A and 55 % B over 40 min, followed by an isocratic phase. Here, A represented hexane, while B was a mixture of hexane and iPrOH (97:3 vol:vol with 10 mmol L^{-1} ammonium acetate). The flow rate, column temperature, and injection volume were 0.45 mL min^{-1}, 24 °C, and 10 µL, respectively. All other conditions matched those used for RP-LC. There is no commercially available standard for extended archaeol, and therefore only the optical rotation of each peak is shown in supplementary Fig. S4 without identifying whether it is the *R* or *S* enantiomer.

2.6. Optical rotation

The optical rotation of the separated peaks of archaeol isomers, see supplementary Table S2, was measured using a JASCO P-2000 polarimeter (JASCO UK Limited, Heckmondwike, West Yorkshire, England).

2.7. Bioinformatics

To explore publicly available genomic resources, we searched for evidence of the presence of genes that encoded G1PDH and G3PDH in the different archaeal taxa (species) used in this study through GenBank (https://www.ncbi.nlm.nih.gov/protein/) and UniProt (https://www.uniprot.org/). To this end, the search combined the textual descriptor of the gene ("glycerol-1-phosphate dehydrogenase" or "glycerol-3-phosphate dehydrogenase") and the species name of the respective archaeon. Prediction of G1PDH and G3PDH for the identified enzymes was performed using HHpred (https://toolkit.tuebingen.mpg.de/tools/hhpred) with searches performed against the Pfam-A v37.4, COG_KOG v1.0, NCBI Conserved Domains (CD) v3.19 and TIGRFAMs v15.0 databases. Multiple sequence alignment was done with Jalview. G3PDH alignments were omitted due their high structural diversity that prevented reliable alignment.

3. Results and discussion

3.1. Biosynthetic pathways

All investigated organisms possess a single copy of the enzyme G1PDH, as confirmed by re-blasting of their respective genomes. These enzymes showed high sequence similarity and contained conserved residues, including those responsible for the Rossmann fold, as well as those involved in zinc-ion and substrate binding [33] (see supplementary Fig. S5 for more details). H. volcanii encodes two putative operons associated with the activity of G3PDH, namely glpA1B1C1 (HVO_1538 to HVO_1540), located on the chromosome near the glycerol kinase gene (glpK), and glpA2B2C2 (HVO_A0269 to HVO_A0271), situated on the pHV4 megaplasmid pHV4 [34]. This enzymatic machinery closely resembles the bacterial counterpart.

S. acidocaldarius was shown to encode two operons of glycerol kinase (GK) and G3PDH (saci_1117 to 1119 and saci_2031 to 2033) involved in the utilization of glycerol. The G3PDH enzyme has an unusual membrane anchoring via a CoxG-like protein, highlighting a unique archaeal adaptation in glycerol metabolism [20]. Comparative BLAST analysis between *S. acidocaldarius* and *S. solfataricus* showed that the enzymes involved in glycerol metabolism had close homologues in *S. solfataricus,* ranging from 70.9 % and 69.6 % for two identified GK (SSO1600 and SSO2133), to 67.7 % for G3PDH (SSO2526), as well as 54.9 % sequence identity for a putative CoxG-like protein (SSO2524). Interestingly, homologs of the two enzymes discussed here were also identified in *M. sedula,* which encodes them within a single operon (Msed_1177; 59.4 % sequence identity to *S. acidocaldarius,* and a CoxG-like Msed_1176 protein showing 44.1 % identity). Although *M. sedula* belongs to the same order of Sulfolobales, the GK gene appears to be absent, suggesting that this organism is not able to utilize glycerol as a carbon source.

The enzyme domains for the corresponding proteins were confirmed: cd08173 for G1PDH and COG0578 for G3PDH in Sulfolobales. In *H. volcanii*, the presence of TIGR03377, COG3075, and TIGR03379 domains was verified, further proving that the correct enzymes were identified. Additionally, *S. acidocaldarius* and *S. solfataricus* possess two additional candidate genes (Saci_2273 and SSO2643) that possibly encapsulate an anaerobic G3PDH chain C (domain: TIGR03379).

Other genera included in this research, i.e., *Methanopyrus* and *Methanothermobacter*, lack the G3PDH (supplementary Table S1). Thus, in the two latter species, archaeols with an *S* configuration on the glycerol backbone should not be present.

3.2. Shotgun lipidomic

Shotgun analysis of the non-saponifiable fractions obtained by alkaline hydrolysis of total lipids from eight archaeal samples (Table S1) is shown in Fig. 1. Based on published data on the tandem mass ESI^+ of archaeol as $[M+Li]^+$ [32], in which the ion at *m/z* 99 was predominant,

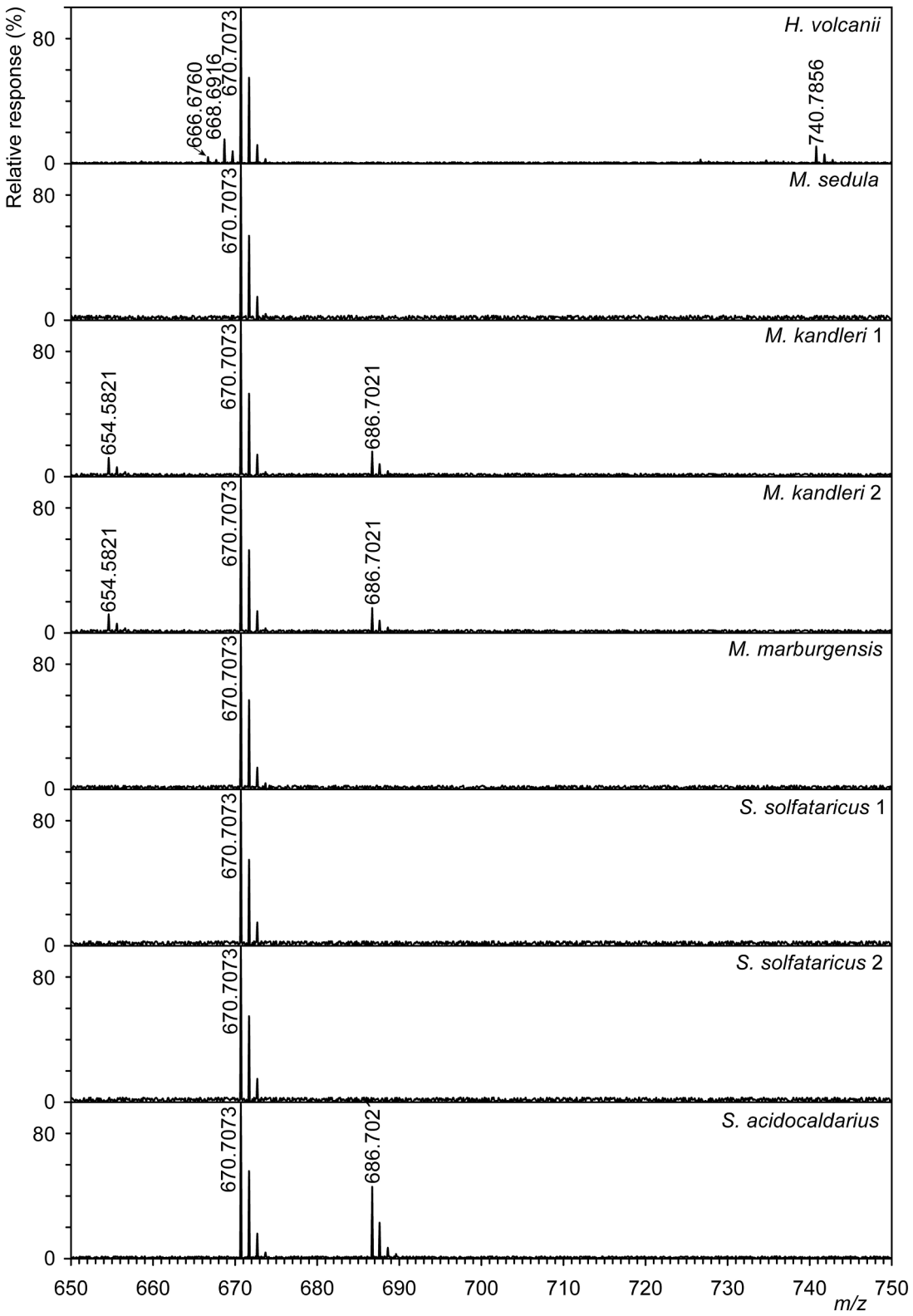

Fig. 1. Shotgun analysis by precursor ion scan (ion with chemical formula: $[C_3H_9O_3]^+$, exact mass: 93.0546) of the different archaea samples detailed in Supplementary Table S1. Only the interval between 650 and 750 Da is shown, i.e. the interval containing archaeol, unsaturated archaeols, hydroxyarchaeols, and extended archaeols.

we identified the ion at *m/z* 93 in ESI^+ spectra of archaeol detected as $[M+H]^+$ and therefore selected it as the precursor ion. An advantage of this ion is that its intensity increases with increasing numbers of C=C double bonds, whereas the relative abundance of the corresponding molecular species decreases. In addition to fully saturated archaeol, minor amounts of unsaturated archaeols were detected in *H. volcanii*, with monounsaturated archaeol constituting ~15 % of the total ($[M+NH_4]^+$, 668.6916 Da). Extended archaeol (C20–C25) was also

observed at *m/z* 740.7856 in the same strain (i.e., *H. volcanii*), along with trace levels of unsaturated analogues. Fig. 1 displays the total ion current over 650–750 Da. In all samples, archaeol was the predominant component (see its tandem mass spectrum in Fig. 2 and the predicted ion structure in supplementary Fig. S6). Archaeols containing one or more double bonds (i.e., molecular masses 668.7, 666.7, and 654.6 Da) were additionally identified in *H. volcanii* and *M. kandleri*, while hydroxyarchaeol (i.e., molecular mass 686.7 Da) was detected as a minor constituent in *M. kandleri* and *S. acidocaldarius* (Fig. 1). Finally, *H. volcanii* contained a higher archaeol homologue, 2-*O*-sesterpanyl-3-*O*-phytanyl-*sn*-glycerol, with side chains C20 and C25, whose tandem mass spectrum and predicted ion structure are shown in supplementary Fig. S6. Furthermore, tetraethers such as GDGT, OH-GDGT, and related compounds were detected in the core lipids, both in saturated and unsaturated forms. However, these compounds were not further identified because they were not required for subsequent analyses.

Published studies describing the presence or absence of archaeol derivatives vary considerably. For example, in *H. volcanii*, several authors [27,35,36] generally agree that this species contains unsaturated archaeols with up to eight double bonds, i.e., 2,3-bis-*O*-(3,7,11,15-tetraenophytanyl)-*sn*-glycerol (2,3-di-*O*-geranylgeranyl-*sn*-glycerol or archaeol C40:8).

A homologue of archaeol, *O*-phytanyl-*O*-sesterterpanyl-*sn*-glycerol (C20–C25-AR), has been reported in Halobacteriales [37], although published results are inconsistent. The presence of extended archaeol was confirmed by Yao et al. [36]. On the contrary, Teixidor et al. [38] and Dawson et al. [28] reported that *H. volcanii* and other species of *Haloferax* did not contain *O*-phytanyl-*O*-sesterterpanyl-*sn*-glycerol, according to GC-MS analyses of trimethyl silyl derivatives.

Similarly, both fully unsaturated archaeol (archaeol C40:8) [39] and hydroxyarchaeol [40] have been reported in *M. kandleri*. Hydroxyarchaeol has also been described in *S. acidocaldarius*, which is consistent with the results presented in Fig. 1. On the contrary, it was not detected in *H. volcanii* in the analyses reported here. Discrepancies between published results may be due to differences in strains used, cultivation conditions, or analytical methodology (GC–MS vs. LC–MS).

3.3. Analysis of archaeols by two-dimensional on-line LC-tandem MS

For further analysis by RP-HPLC/MS-ESI$^+$, *H. volcanii* was selected mainly because it yielded the highest amount of biomass and is among the archaeal strains that are the most easily grown in the laboratory [41]. Using RP-HPLC/MS-ESI$^+$, it was proven that *H. volcani* contained both saturated and unsaturated archaeols, as well as their homologues (extended archaeols). Archaeol (C20-C20-AR) with a retention time of 37.75 min (Fig. 3) was identified as the major peak, see tandem MS in Fig. 2. Furthermore, unsaturated archaeols were identified, e.g. C20:2-C20:0-AR having tR = 35.13 min or C20:1-C20:0-AR (tR = 36.27 min). In particular, it was confirmed here that *H. volcanii* contained not only fully saturated extended archaeol (with tR = 47.84 min), but also molecular species that have tR = 42.46 min with 7 double bonds, see $[M+NH_4]^+$ at *m/z* 726.6761 (C20:3-C25:4-AR) (Fig. 3). At the same time, the presence of bis-extended archaeol, i.e. di-sesterpanyl (C25-C25) archaeol, was not confirmed. If present, it was at concentrations at least two orders of magnitude lower than the C20-C20 archaeol, see again Fig. 3. This double homolog was, for example, identified in other Archaea such as *Aeropyrum pernix* [42], *Methanomassiliicoccus luminyensis* [43] or in samples of solar evaporation pond liquor [16].

The chromatogram corresponding to archaeol purchased from Avanti separated four peaks corresponding to four isomers (Fig. 4). Using chiral HPLC, the purities were estimated to be 1.1 % for probably (*S*)-2,3-bis((3*S*,7*R*,11*R*)-3,7,11,15-tetramethylhexadecyl)oxy)propan-1-ol, 10.7 % for (*S*)-2,3-bis(((3*R*,7*R*,11*R*)-3,7,11,15-tetramethylhexadecyl)oxy)propan-1-ol, 4.3 % for (*R*)-2,3-bis(((3*S*,7*R*,11*R*)-3,7,11,15-

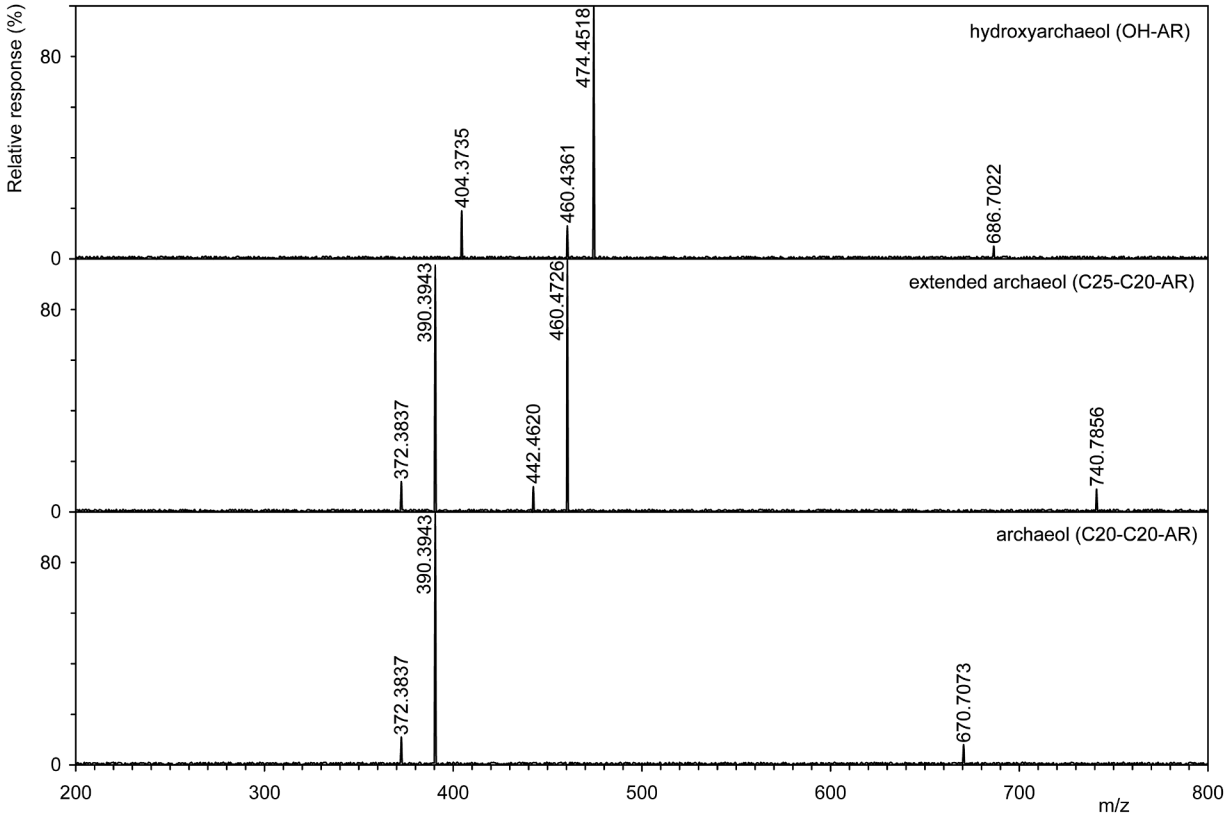

Fig. 2. Tandem mass spectra of three major diethers (archaeol, extended archaeol, and hydroxyarchaeol) identified in the samples reported in this study.

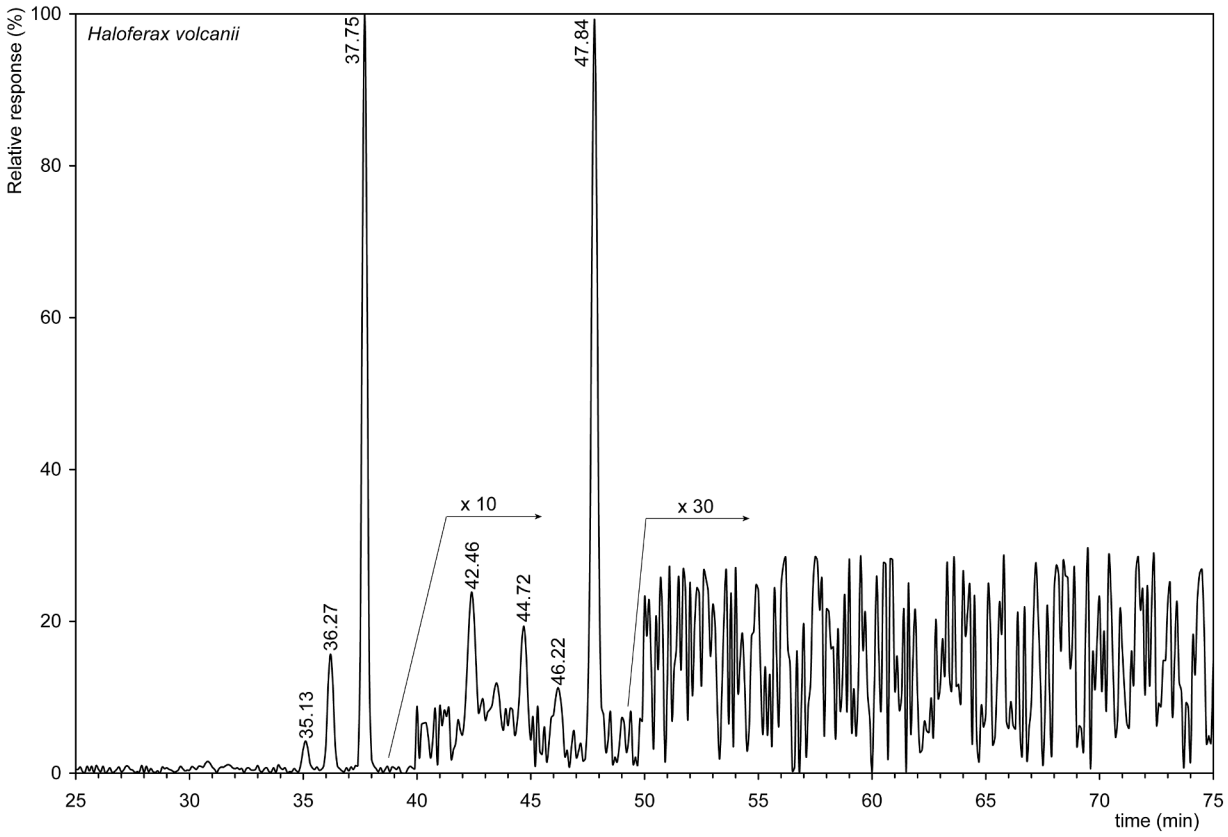

Fig. 3. Reverse phase separation of the mixture of archaeol derivatives from *Haloferax volcani* (unsaturated and saturated derivatives of archaeols and/or extended archaeols) in three reverse phase columns connected in series. The main peaks (tR) identified by tandem mass spectrometry are as follows: unsaturated archaeols (tR = 35.13 and 36.27 min), archaeol (tR = 37.75), extended unsaturated archaeols (tR = 42.46, 44.72, and 46.22 min), and extended archaeol (tR = 47.84 min).

tetramethylhexadecyl)oxy)propan-1-ol, and 83.9 % for (*R*)-2,3-bis (((3*R*,7*R*,11*R*)-3,7,11,15-tetramethylhexadecyl)oxy)propan-1-ol.
Archaeols with abundances of 1.1 % and 4.3 % most likely had a different configuration from the others, potentially at C_3 of the phytyl unit [11,44]. Their optical rotations are listed in supplementary Table S2.

The peak with the highest abundance, i.e. the peak with tR = 32.66 min, was identified based on tR, tandem MS, and optical rotation. Various authors report $[\alpha]_D$ ranging from +7.1 to +9.68°, see note b in supplementary Table S2. This confirmed the stereochemistry of the *R* archaeol. Supplementary Fig. S7 describes the tandem mass spectra of both epimers, and it is evident that these spectra are identical.

The identity of the further enantiomer with tR = 31.67 min, i.e., (*S*)-2,3-bis(((3*R*,7*R*,11*R*)-3,7,11,15-tetramethylhexadecyl)oxy) propan-1-ol, referred to in the article by Morii et al. [45] as 1,2-di-*O*-p-hytanyl-*sn*-glycerol, was established by the $[\alpha]_D$. Morii et al. reported $[\alpha]_D$ -7.1°, which confirmed the stereostructure, which was also set in the article by Kates [13]. Our value of $[\alpha]_D$ -8.06 is given in supplementary Table S2.

Two more isomers were also identified, one with a tR of 31.11 min and the other with a tR of 32.04 min. While the latter was present in sufficient quantity to measure the optical rotation $[\alpha]_D$ = 7.19, the earlier was not. On the basis of published data, it can be assumed that the isomer with a tR of 32.04 min is the isomer with a different configuration at C_3 (*S*), which is also consistent with its optical rotation (see supplementary Table S2 for details). Régnier et al. [11] also found the corresponding isomer (*S*-archaeol with tR = 123.614 min) by ion scanning at *m/z* 760.65, but unfortunately, the authors did not identify it further. In our case, this peak had a tR of 31.11 min. This isomer has an abundance of approximately 1.25 % of the *R* isomer, and because it is a minority, the optical rotation could not have been measured here. Its probable stereoisomerism was inferred from tR alone. To determine the configuration of the seven asymmetric centers, a larger amount of archaeol would have to be obtained, which we were unable to do with the 5 mg purchased from Avanti. Furthermore, this isomer was not identified in any of the eight cultivated biological samples reported here.

However, it should be noted that the separation of all the 128 theoretically existing synthesized isomers of archaeol is very poor; see Fig. S17 from the paper by Régnier et al. [11]. However, the authors attempted to estimate the representation of (*R*)-2,3-bis(((3*R*,7*R*,11*R*)-3,7,11,15-tetramethylhexadecyl)oxy)propan-1-ol, which, according to their calculation, was 6.46 % of total isomers. On the basis of all of the above results, we assume that four of the six cultured strains analyzed here contained both the *R* and *S* enantiomers of archaeol. The *S* enantiomer always represented a minority of archaeols, its share varying according to the corresponding strain from 6.8 to 13.9 % of the *R* enantiomer (supplementary Table S2). This result is consistent with previously published results [21] and with the evidence obtained from the GenBank database and through the bioinformatic analyses reported above, i.e., strains without evidence of G3PDH in their genomes (*Methanopyrus* and *Methanothermobacter)* also lacking biochemical evidence for *S* enantiomers of archaeol upon analyzing their lipids.

4. Conclusion

Based on all of the results obtained by chiral chromatography, it seems very likely that some genera and species of Archaea can biosynthesize two enantiomers of archaeol. These results are in good agreement with mounting evidence that in addition to the homochiral membranes of Bacteria [9,46] and in Archaea, both G1P and G3P can be present as starter units in some of the archaeal taxa. The stereochemical partitioning of the lipids thus is not as strict as originally thought,

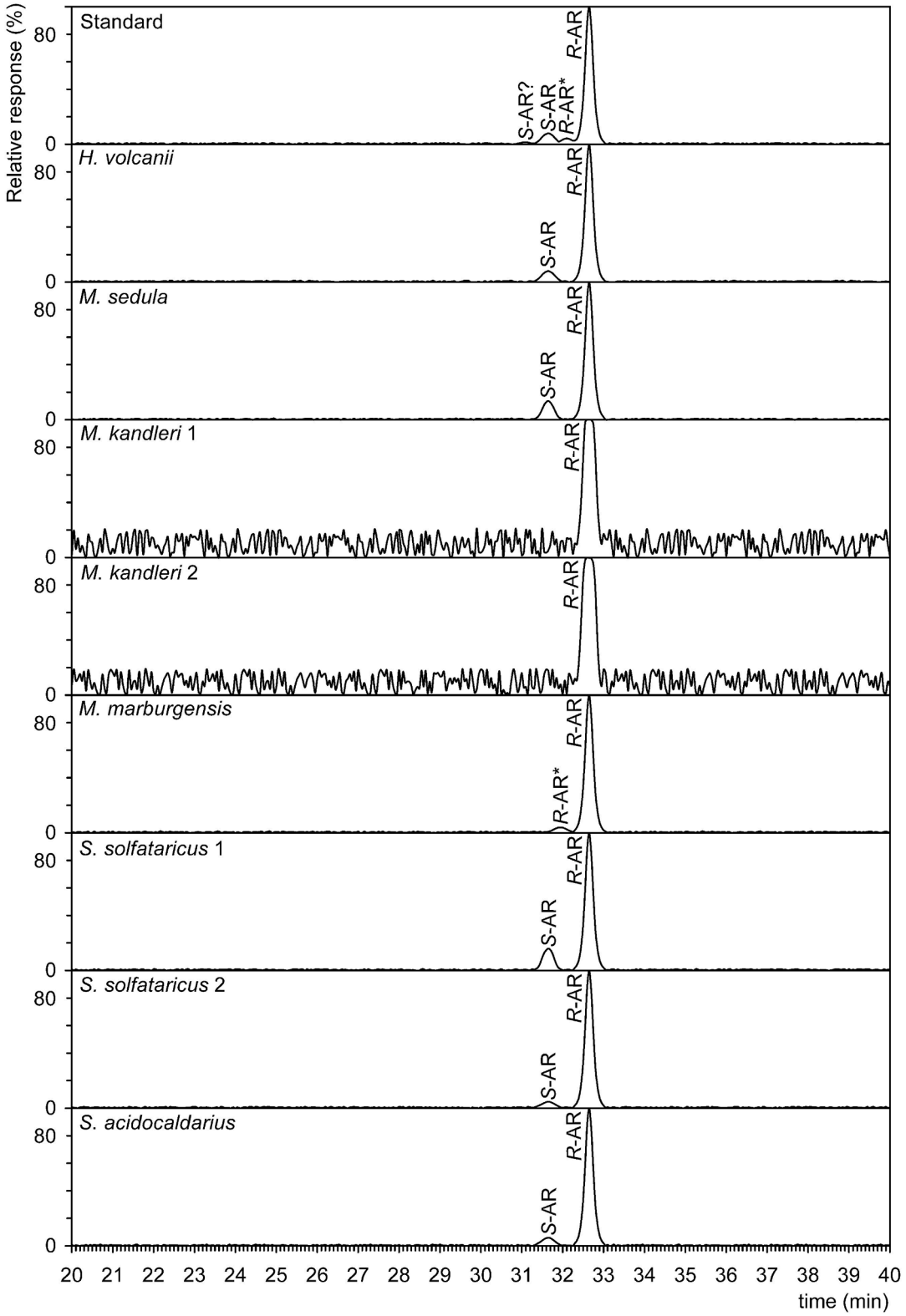

Fig. 4. Separation of archaeol from six strains of Archaea and the commercial standard obtained by analysis on two chiral columns connected in series. *R*-AR = (*R*)-2,3-bis(((3*R*,7*R*,11*R*)-3,7,11,15-tetramethylhexadecyl)oxy)propan-1-ol, *R*-AR* = (*R*)-2,3-bis(((3*S*,7*R*,11*R*)-3,7,11,15-tetramethylhexadecyl)oxy)propan-1-ol, *S*-AR = (*S*)-2,3-bis(((3*R*,7*R*,11*R*)-3,7,11,15-tetramethylhexadecyl)oxy)propan-1-ol, *S*-AR? = probably (*S*)-2,3-bis(((3*S*,7*R*,11*R*)-3,7,11,15-tetramethylhexadecyl)oxy)propan-1-ol.

including the presence of genes related to G1P and G3P in bacterial [46–48] and archaeal [49] genomes, as well as detection of both G1P and G3P in genetically modified *E. coli* [7] and several Gram-positive Bacteria [9]. For example, in *S. acidocaldarius*, glycerol is phosphorylated to glycerol-3-phosphate by GK [20]. Therefore, the resulting G3P can be involved in the biosynthesis of archaeols as the backbone, in addition to G1P. The genome of the hyperthermophilic archaeon *Archaeoglobus fulgidus* contains a G3PDH ortholog (*gps*A), and biochemical characterization demonstrated G3PDH-like activity of the recombinant *gps*A gene product [19].

The stability of heterochiral hybrid membranes composed of bacterial polar lipids of type *sn*-G3P and archaeal polar lipids of type *sn*-G1P was previously investigated [5]. The results demonstrated that heterochiral hybrid liposomes exhibited stability comparable to that of homochiral liposomes, suggesting that such hybrid membranes can be as robust as the biomembranes of contemporary thermophilic microorganisms. These findings support the notion that heterochiral membranes were already present during the early evolution of life, likely serving as lipid components of LUCA before the divergence of Archaea and Bacteria, and remnants of these structures may still persist in extant microorganisms under certain conditions. To fully confirm this hypothesis, that is, that some Archaea have heterochiral membranes, further analysis is necessary, focusing either on archaeol isomers and/or isolation and identification of the relevant genes/enzymes using advanced genomic or proteomic tools.

Data availability

Primary data is deposited in Zenodo (doi: 10.5281/zenodo.17485876).

Funding

The research was supported by the Institutional Research Concept RVO 61388971 (Institute of Microbiology, Prague, Czech Republic), the Ministry of Education, Youth and Sports of the Czech Republic (CZ.02.01.01/00/22_008/0004597, Talking Microbes – Understanding Microbial Interactions within One Health Framework). N.P. was supported by the Austrian Science Fund (FWF) Elise Richter Fellowship (FWF project V 931-B).

Declaration of generative AI and AI-assisted technologies in the writing process

During the preparation of this work, the authors used ChatGPT in order to improve English language and style. After using this tool/service, the authors reviewed and edited the content as needed and assume full responsibility for the content of the publication.

CRediT authorship contribution statement

Walter Hofmann: Writing – review & editing, Methodology, Investigation. **Andrea Palyzová:** Writing – review & editing, Writing – original draft, Visualization, Investigation, Funding acquisition. **Jan Jansa:** Writing – review & editing, Visualization, Methodology. **Nika Pende:** Writing – review & editing, Methodology. **Simon K.-M.R. Rittmann:** Writing – review & editing, Validation, Supervision, Resources, Methodology. **Tomáš Řezanka:** Writing – review & editing, Validation, Supervision, Resources, Investigation, Data curation, Conceptualization.

Declaration of competing interest

The authors declare that they have no known competing financial interests or personal relationships that could have appeared to influence the work reported in this paper.

Supplementary materials

Supplementary material associated with this article can be found, in the online version, at doi:10.1016/j.chroma.2026.466853.

References

[1] V. Sojo, On the biogenic origins of homochirality, Orig. Life Evol. Biosph. 45 (2015) 219–224, https://doi.org/10.1007/s11084-015-9422-9.
[2] N. Suzuki, Y. Itabashi, Possible roles of amphiphilic molecules in the origin of biological homochirality, Symmetry 11 (2019) 966, https://doi.org/10.3390/sym11080966.
[3] I.B. Jeffery, M.J. Claesson, P.W. O'Toole, F. Shanahan, Categorization of the gut microbiota: enterotypes or gradients? Nat. Rev. Microbiol. 10 (2012) 591–592, https://doi.org/10.1038/nrmicro2859.
[4] I. Mizrahi, R.J. Wallace, S. Moraïs, The rumen microbiome: balancing food security and environmental impacts, Nat. Rev. Microbiol. 19 (2021) 553–566, https://doi.org/10.1038/s41579-021-00543-6.
[5] H. Shimada, A. Yamagishi, Stability of heterochiral hybrid membrane made of bacterial sn-G3P lipids and archaeal sn-G1P lipids, Biochemistry 50 (2011) 4114–4120, https://doi.org/10.1021/bi200172d.
[6] T. Šantl-Temkiv, P. Amato, E.O. Casamayor, P.K.H. Lee, S.B. Pointing, Microbial ecology of the atmosphere, FEMS Microbiol. Rev. 46 (2022) fuac009, https://doi.org/10.1093/femsre/fuac009.
[7] A. Caforio, M.F. Siliakus, M. Exterkate, S. Jain, V.R. Jumde, R.L.H. Andringa, S.W. M. Kengen, A.J. Minnaard, A.J.M. Driessen, J. van der Oost, Converting *Escherichia coli* into an Archaebacterium with a hybrid heterochiral membrane, Proc. Natl. Acad. Sci. U. S. A. 115 (2018) 3704–3709, https://doi.org/10.1073/pnas.1721604115.
[8] V. Petrenko, F. Sinturel, H. Riezman, C. Dibner, Lipid metabolism around the body clocks, Prog. Lipid Res. 91 (2023) 101235, https://doi.org/10.1016/j.plipres.2023.101235.
[9] A. Palyzová, I.A. Guschina, T. Řezanka, Chiral analysis of glycerol phosphates - can bacteria biosynthesize heterochiral phospholipid membranes? J. Chromatogr. A 1676 (2022) 463267 https://doi.org/10.1016/j.chroma.2022.463267.
[10] R.J. Parkes, G. Webster, B.A. Cragg, A.J. Weightman, C.J. Newberry, T. G. Ferdelman, J. Kallmeyer, B.B. Jørgensen, I.W. Aiello, J.C. Fry, Deep sub-seafloor prokaryotes stimulated at interfaces over geological time, Nature 436 (2005) 390–394, https://doi.org/10.1038/nature03796.
[11] S. Régnier, E. Lam, V. Vasquez, C.F. Martinez-Farina, F.C. Stark, G. Agbayani, L. Deschatelets, R. Dudani, B.A. Harrison, B. Akache, M.J. McCluskie, U.D. Hemraz, Effect of chiral purity on adjuvanticity of Archaeol-based glycolipids, J. Med. Chem. 65 (2022) 8332–8344, https://doi.org/10.1021/acs.jmedchem.2c00072.
[12] T. Řezanka, L. Kyselová, D.J. Murphy, Archaeal lipids, Prog. Lipid Res. 91 (2023) 101237, https://doi.org/10.1016/j.plipres.2023.101237.
[13] M. Kates, The phytanyl ether-linked polar lipids and isoprenoid neutral lipids of extremely halophilic bacteria, Prog. Chem. Fats Other Lipids 15 (1977) 301–342, https://doi.org/10.1016/0079-6832(77)90011-8.
[14] T. Li, Y. Luo, C. Liu, X. Lu, B. Feng, Archaeal lipids: extraction, separation, and identification via natural product chemistry perspective, Int. J. Mol. Sci. 26 (2025) 3167, https://doi.org/10.3390/ijms26073167.
[15] M.F. Siliakus, J. van der Oost, S.W.M. Kengen, Adaptations of archaeal and bacterial membranes to variations in temperature, pH and pressure, Extremophiles 21 (2017) 651–670, https://doi.org/10.1007/s00792-017-0939-x.
[16] M. de Rosa, A. Gambacorta, B. Nicolaus, W.D. Grant, A C_{25},C_{25} diether core lipid from Archaebacterial Haloalkaliphiles, Microbiology 129 (1983) 2333–2337, https://doi.org/10.1099/00221287-129-8-2333.
[17] G.L.S. Liman, A.A. Garcia, K.A. Fluke, H.R. Anderson, S.C. Davidson, P. V. Welander, T.J. Santangelo, Tetraether archaeal lipids promote long-term survival in extreme conditions, Mol. Microbiol. 121 (2024) 882–894, https://doi.org/10.1111/mmi.15240.
[18] Y. Koga, H. Morii, Biosynthesis of ether-type polar lipids in Archaea and evolutionary considerations, Microbiol. Mol. Biol. Rev. 71 (2007) 97–120, https://doi.org/10.1128/mmbr.00033-06.
[19] S. Sakasegawa, C.H. Hagemeier, R.K. Thauer, L.O. Essen, S. Shima, Structural and functional analysis of the *gpsA* gene product of *Archaeoglobus fulgidus*: a glycerol-3-phosphate dehydrogenase with an unusual NADP+ preference, Protein Sci. 13 (2004) 3161–3171, https://doi.org/10.1110/ps.04980304.
[20] C. Schmerling, C. Schroeder, X. Zhou, J. Bost, B. Waßmer, S. Ninck, T. Busche, L. Montero, F. Kaschani, O.J. Schmitz, J. Kalinowski, M. Kaiser, S.-V. Albers, C. Bräsen, B. Siebers, An unusual glycerol-3-phosphate dehydrogenase in *Sulfolobus acidocaldarius* elucidates the diversity of glycerol metabolism across Archaea, Commun. Biol. 8 (2025) 539, https://doi.org/10.1038/s42003-025-07953-9.
[21] M. Nishihara, T. Yamazaki, T. Oshima, Y. Koga, sn-glycerol-1-phosphate-forming activities in Archaea: separation of archaeal phospholipid biosynthesis and glycerol catabolism by glycerophosphate enantiomers, J. Bacteriol. 181 (1999) 1330–1333, https://doi.org/10.1128/jb.181.4.1330-1333.1999.
[22] S. Lee, S.J. Kim, E. Bang, Y.C. Na, Chiral separation of intact amino acids by capillary electrophoresis-mass spectrometry employing a partial filling technique with a crown ether carboxylic acid, J. Chromatogr. A 1586 (2019) 128–138, https://doi.org/10.1016/j.chroma.2018.12.001.
[23] M.J. Boundy, A.I. Selwood, D.T. Harwood, P.S. McNabb, A.D. Turner, Development of a sensitive and selective liquid chromatography–mass spectrometry method for high throughput analysis of paralytic shellfish toxins using graphitised carbon solid

phase extraction, J. Chromatogr. A. 1387 (2015) 1–12, https://doi.org/10.1016/j.chroma.2015.01.086.
[24] W. Lyu, B. Yuan, F.F. Dinssa, J.E. Simon, Q. Wu, Rapid screening of glycoalkaloids in *Solanum scabrum* and *S. nigrum* berries using ultra-high-performance liquid chromatography with pathway-specified in-source fragmentation tandem mass spectrometry, Rapid Commun. Mass Spectrom. 34 (2020) e8882, https://doi.org/10.1002/rcm.8882.
[25] D.J. Bernstein, T. Lange, Post-quantum cryptography, Nature 549 (2017) 188–194, https://doi.org/10.1038/nature23461.
[26] E.G. Bligh, W.J. Dyer, A rapid method of total lipid extraction and purification, Can. J. Biochem. Physiol. 37 (1959) 911–917, https://doi.org/10.1139/o59-099.
[27] C. Kropp, J. Lipp, A.L. Schmidt, C. Seisenberger, M. Linde, K.-U. Hinrichs, P. Babinger, Identification of acetylated diether lipids in halophilic Archaea, MicrobiologyOpen 11 (2022) e1299, https://doi.org/10.1002/mbo3.1299.
[28] K.S. Dawson, K.H. Freeman, J.L. Macalady, Molecular characterization of core lipids from halophilic Archaea grown under different salinity conditions, Org. Geochem. 48 (2012) 1–8, https://doi.org/10.1016/j.orggeochem.2012.04.003.
[29] S. Horai, N. Yamauchi, H. Naraoka, Simultaneous total analysis of core and polar membrane lipids in Archaea by high-performance liquid chromatography/high-resolution mass spectrometry coupled with heated electrospray ionization, Rapid Commun. Mass Spectrom. 33 (2019) 1571–1577, https://doi.org/10.1002/rcm.8506.
[30] C. Zhu, J.S. Lipp, L. Wörmer, K.W. Becker, J. Schröder, K.-U. Hinrichs, Comprehensive glycerol ether lipid fingerprints through a novel reversed phase liquid chromatography–mass spectrometry protocol, Org. Geochem. 65 (2013) 53–62, https://doi.org/10.1016/j.orggeochem.2013.09.012.
[31] D. Birgel, A. Guido, X. Liu, K.-U. Hinrichs, S. Gier, J. Peckmann, Hypersaline conditions during deposition of the Calcare di Base revealed from archaeal di- and tetraether inventories, Org. Geochem. 77 (2014) 11–21, https://doi.org/10.1016/j.orggeochem.2014.09.002.
[32] L.M. de Souza, M. Muller-Santos, M. Iacomini, P.A.J. Gorin, G.L. Sassaki, Positive and negative tandem mass spectrometric fingerprints of lipids from the halophilic Archaea *Haloarcula marismortui*, J. Lipid Res. 50 (2009) 1363–1373, https://doi.org/10.1194/jlr.M800478-JLR200.
[33] J.S. Han, K. Ishikawa, Active site of Zn(2+)-dependent sn-glycerol-1-phosphate dehydrogenase from *Aeropyrum pernix* K1, Archaea (Vancouver, B.C.) 1 (2005) 311–317, https://doi.org/10.1155/2005/257264.
[34] K.S. Rawls, J.H. Martin, J.A. Maupin-Furlow, Activity and transcriptional regulation of bacterial protein-like glycerol-3-phosphate dehydrogenase of the Haloarchaea in *Haloferax volcanii*, J. Bacteriol. 193 (2011) 4469–4476, https://doi.org/10.1128/jb.00276-11.
[35] T. Stiehl, J. Rullkötter, A. Nissenbaum, Molecular and isotopic characterization of lipids in cultured halophilic microorganisms from the Dead Sea and comparison with the sediment record of this hypersaline lake, Org. Geochem. 36 (2005) 1242–1251, https://doi.org/10.1016/j.orggeochem.2005.05.002.
[36] W. Yao, W. Zhang, W. He, W. Xiao, Y. Chen, Y. Zhu, F. Zheng, C. Zhang, Lipidomic chemotaxonomy aligned with phylogeny of Halobacteria, Front. Microbiol. 14 (2023) 1297600, https://doi.org/10.3389/fmicb.2023.1297600.
[37] L. Villanueva, J.S.S. Damsté, S. Schouten, A re-evaluation of the archaeal membrane lipid biosynthetic pathway, Nat. Rev. Microbiol. 12 (2014) 438–448, https://doi.org/10.1038/nrmicro3260.
[38] P. Teixidor, J.O. Grimait, J.J. Pueyo, F. Rodriguez-Valera, Isopranylglycerol diethers in non-alkaline evaporitic environments, Geochim. Cosmochim. Acta 57 (1993) 4479–4489, https://doi.org/10.1016/0016-7037(93)90497-K.
[39] D. Hafenbradl, M. Keller, R. Thiericke, K.O. Stetter, A novel unsaturated archaeal ether core lipid from the hyperthermophile *Methanopyrus kandleri*, Syst. Appl. Microbiol. 16 (1993) 165–169, https://doi.org/10.1016/S0723-2020(11)80463-7.
[40] G.D. Sprott, B.J. Agnew, G.B. Patel, Structural features of ether lipids in the archaeobacterial thermophiles *Pyrococcus furiosus, Methanopyrus kandleri, Methanothermus fervidus*, and *Sulfolobus acidocaldarius*, Can. J. Microbiol. 43 (1997) 467–476, https://doi.org/10.1139/m97-066.
[41] M. Rafiq, N. Hassan, M. Rehman, M. Hayat, G. Nadeem, F. Hassan, N. Iqbal, H. Ali, S. Zada, Y. Kang, W. Sajjad, M. Jamal, Challenges and approaches of culturing the unculturable Archaea, Biology 12 (2023) 1499, https://doi.org/10.3390/biology12121499.
[42] J. Genova, N.P. Ulrih, V. Kralj-Iglič, A. Iglič, I. Bivas, Bending elasticity modulus of giant vesicles composed of *Aeropyrum pernix* K1 Archaeal lipid, Life 5 (2015) 1101–1110, https://doi.org/10.3390/life5021101.
[43] K.W. Becker, F.J. Elling, M.Y. Yoshinaga, A. Söllinger, T. Urich, K.-U. Hinrichs, Unusual butane- and pentanetriol-based tetraether lipids in *Methanomassiliicoccus luminyensis*, a representative of the seventh order of methanogens, Appl. Environ. Microbiol. 82 (2016) 4505–4516, https://doi.org/10.1128/AEM.00772-16.
[44] U.D. Hemraz, E. Lam, V. Vasquez, F.C. Stark, B. Akache, Mixture of stereoisomers of a sulfated glycolipid, Patent No. WO_2023131849_A1 (2023).
[45] H. Morii, T. Eguchi, Y. Koga, In vitro biosynthesis of ether-type glycolipids in the Methanoarchaeon *Methanothermobacter thermautotrophicus*, J. Bacteriol. 189 (2007) 4053–4061, https://doi.org/10.1128/jb.01875-06.
[46] L. Villanueva, F.A.B. von Meijenfeldt, A.B. Westbye, S. Yadav, E.C. Hopmans, B. E. Dutilh, J.S.S. Damsté, Bridging the membrane lipid divide: Bacteria of the FCB group superphylum have the potential to synthesize archaeal ether lipids, Isme J 15 (2021) 168–182, https://doi.org/10.1038/s41396-020-00772-2.
[47] H. Guldan, R. Sterner, P. Babinger, Identification and characterization of a bacterial glycerol-1-phosphate dehydrogenase: Ni^{2+}-dependent AraM from *Bacillus subtilis*, Biochemistry 47 (2008) 7376–7384, https://doi.org/10.1021/bi8005779.
[48] H. Guldan, F.-M. Matysik, M. Bocola, R. Sterner, P. Babinger, Functional assignment of an enzyme that catalyzes the synthesis of an Archaea-type ether lipid in bacteria, Angew. Chem. Int. Ed. 50 (2011) 8188–8191, https://doi.org/10.1002/anie.201101832.
[49] G.A. Coleman, R.D. Pancost, T.A. Williams, Investigating the origins of membrane phospholipid piosynthesis genes using outgroup-free rooting, Genome Biol. Evol. 11 (2019) 883–898, https://doi.org/10.1093/gbe/evz034.